CH_3F SUBMILLIMETER LASER USING NEW TYPE OF RESONATOR

Y. Kokubo and M. Kawamura

Department of Physical Electronics
Tokyo Institute of Technology
Ookayama, Meguro-ku, Tokyo

Abstract

A new type of resonator consisting of two metallic circular disks and a cylinder was applied as a guided cavity to the CH_3F laser with successful operation.

Introduction

The development of the optically pumped lasers[1] is dissolving the lack of good sources in submillimeter waves region. Among them the CH_3F laser is well known. Authors have reported[2] on the CH_3F laser using a metallic circular waveguide and pointed out that this laser is very effective for obtaining medium power of 496 μm in wavelength, but that it has defects such as it is long in its essential structure and also the Stark electric field will not be applied due to mechanical structure.

In this paper we present on the CH_3F laser using a new type of resonator which doesn't have the above mentioned faults.

Theory

Figure 1 shows the energy levels of CH_3F molecules concerned with the 496 μm transition. CH_3F molecules, as well known, absorb 9.55 μm line which is very close to 9P (20) line in wavelength in the CO_2 laser lines, and the transition ^{Q}R (11,2) emits 496 μm Far Infrared.

In figure 2 is shown the fundamental structure of this resonator in cylindrical coordinate (φ, r, Z). This is essentially a cylindrical cavity consisting of an upper and lower circular disk and a cylindrical wall which are all made of conductor. a is the radius of cavity and L is the length of cavity. FIR electromagnetic waves propagate along φ-direction.

Both TE- and TM-mode can be excited in the cavity. But, since TE mode can be propagated in the φ-direction with relatively low transmission loss, this mode only will be considered here in details.

The electric and magnetic field components of TE n, m, l mode can be written as follows.

$$E_r = -A \frac{\omega\mu_0 n}{k_c^2} \frac{J_n(k_c r)}{r} \sin k_z Z \, \epsilon^{-jn\varphi} \quad (1)$$

$$E_\varphi = jA \frac{\omega\mu_0}{k_c^2} J_n'(k_c r) \sin k_z Z \, \epsilon^{-jn\varphi} \quad (2)$$

$$E_Z = 0 \quad (3)$$

$$H_r = A \frac{k_z}{k_c} J_n'(k_c r) \cos k_z Z \, \epsilon^{-jn\varphi} \quad (4)$$

$$H_\varphi = -jA \frac{n k_z}{k_c^2} \frac{J_n(k_c r)}{r} \cos k_z Z \, \epsilon^{-jn\varphi} \quad (5)$$

$$H_Z = A J_n(k_c r) \sin k_z Z \, \epsilon^{-jn\varphi} \quad (6)$$

where

$$k_c^2 + k_z^2 = k_0^2 (= \omega^2 \varepsilon_0 \mu_0) \quad (7)$$

$$J_n'(k_c a) = 0 \quad (8)$$

$$k_z = l\pi/L \quad (9)$$

where A: constant; ω : angular frequency; ε_0, μ_0 : dielectric and permeability constant of vacuum; n, m, l,; numbers of half wavelength along φ, r and Z direction; k_c : cut-off phase constant; $J_n(k_c r)$: Bessel function of n th order; J_n' : differential of Bessel function respecting to ($k_c r$).

In our case, n is very large. So we assume that the electromagnetic waves exist only in the region very close to the side wall of cylinder. In this case the attenuation constant of the mode, α_{TE}, is written in the equation,

$$\alpha_{TE} \simeq \frac{1}{\delta\sigma\omega\mu_0 nL} \left[\frac{nL}{k_c^2 a} \cdot \frac{k_c^2 a^2 + n^2 k_z^2}{k_c - n} + \frac{2n^2 k_z^2}{k_c^2} + \frac{2nk_z^2 a}{k_c} \right] \quad (10)$$

where δ : skin depth; σ : conductivity of the conductor.

A typical result of calculation for the equation (10) is shown in figure 3. The attenuation constant decreases with the decrease of n, with constant diameter. Because FIR will spread gradually inside the cavity as n decreases. Figure 4 shows one example of the FIR output power behavior as a function of the Stark field which is parallel to the electric field of the pumping light.

Experiments

Experimental set-up is shown in figure 5. The pumping light from a tunable CO_2 laser is introduced into the resonator through M1, M2 both gold-evaporated mirrors, and L1, a ZnSe converging lens. A He-Ne laser is used to adjust, in advance, the light path in such a way that the pumping light is introduced properly into the resonator. A GOLAY detector is used for the power measurement of the oscillated FIR.

The vertical and horizontal cross-section of cavity is shown in figure 6. This cavity is constructed by an upper and lower circular metal disks and a conductor cylinder as shown in the figure. The diameter of cylinder is about 20 cm. The tuning of FIR oscillation is done by making the upper disk move through a micrometer attached to it. A slit is made along the periphery of the lower disk. So the output FIR power is extracted through a H-guide prepared below the slit. The separation between the upper and lower disks can be varied 10 mm to 20 mm. This variation corresponds, when used with the adjusted injection angle of pumping wave, to the length change of 10 mm to 20 mm in the case of the conventional straight type waveguide laser.

The tuning characteristics obtained when the injection angle nearly equal 70 degree (depicting an octangular path in one round) and the pumping power is 3 W is shown in figure 7. FIR oscillation occurs with each mirror displacement of 20 to 25 μm. If n in TE n, m, l mode is varied by one according to the change of L, the displacement of mirror, ΔL, is given by

$$\frac{\Delta L}{L} \simeq \pm \left(\sqrt{\frac{a l^2}{a l^2 \pm K L^2}} - 1 \right) \quad (11)$$

where $$K = \sqrt{(2/\lambda)^2 - (l/\lambda)^2} \quad (12)$$

Therefore, the oscillation mode in this case will be $TE_{720,20,30}$.

The pressure dependency of the FIR output power is shown in figure 8. There exists the optimum pressure giving the maximum output power irrespective of the angle of incidence of pumping light. When the pressure is rela-

0149-645X/81/0000-0191$00.75

tively low the FIR output increases with the pressure, because the absorption of IR increases with the density of medium. When the pressure is too high the output decreases with it, because the high pressure brings the reduction of the effect of diffusion of the molecules and the increase of the transition relaxation rate between the rotational energy levels.

There also exists the optimum angle of incidence of the pumping light. When it is too small the FIR output power doesn't become large. Because, since then the pumping light tends to come to the central region of cavity, the density of pumping light having the interaction with FIR field becomes too small. When, on the other hand, the angle of incidence of the pumping light is too big the output power decreases. Because, since then the reflection of pumping light by the side wall of resonator occurs more frequently, the attenuation of pumping light increases.

Figure 9 shows the FIR output power as a function of the Stark field (E_S). Curve (a) means the output power variation in the case that E_S is parallel to the pumping field (E pump) and curve (b) shows that in the case E_S is perpendicular to E pump. In former case, the FIR output power decreases with E_S and in latter case the output power takes a maximum value at a certain Stark field. This results agree approximately with the case of a hybrid guide previously appeared.[3]

Conclusion

A new type of resonator was proposed and a successful operation of CH_3F submillimeter laser using the resonator was achieved. The FIR output power was limited to around 30 μW at this stage. And this value will be increased by the careful design of cavity and the further investigation.

Acknowledgment

Authors like to express their great thanks to I. Masuda and Y. Yamada for their experimental cooperation and to M. Makiuchi for his valuable discussions.

References

1. J. J. Gallagher, et al, "Tabulation of Optically Pumped Far Infrared Laser Lines and Applications to Atmospheric Transmission," Infrared Physics, 17, P. 43 (1977)
2. Y. Kokubo, et al, "CW-CH_3F Metallic Waveguide Laser at 496 μm ," Trans. IECE '81/1 Vol. J64-C, No. 1
3. M. Inguscio, et al, "Electric Field Effects on the Efficiency of Optically Pumped Submillimeter Lasers" IEEE. J. Quantum Electron., 16, 9, P955 (1980)

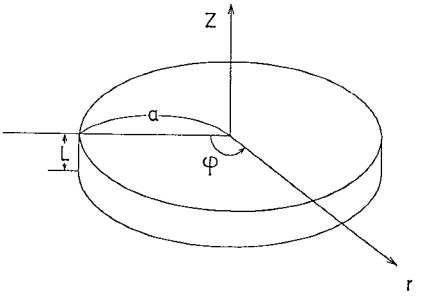

Figure 2. Basic structure of a proposed resonator.

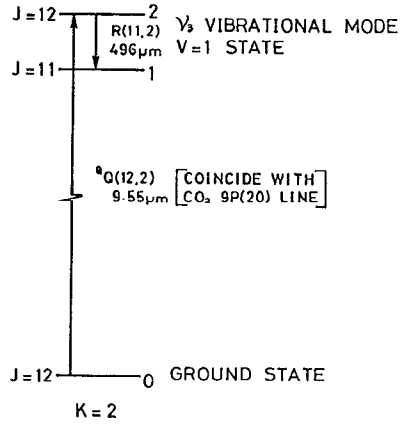

Figure 1. Energy levels of CH_3F molecules.

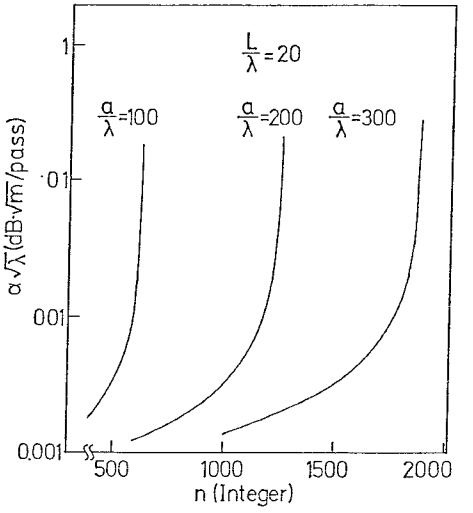

Figure 3. Attenuation constant of the resonator as a function of n (integer).

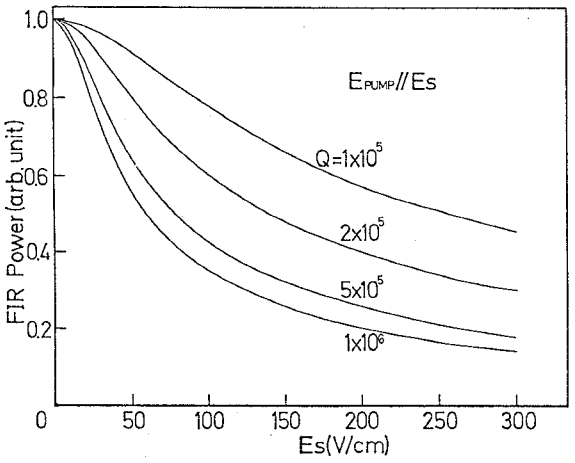

Figure 4. Calculated FIR output power versus Stark field when this is parallel to pumping field.

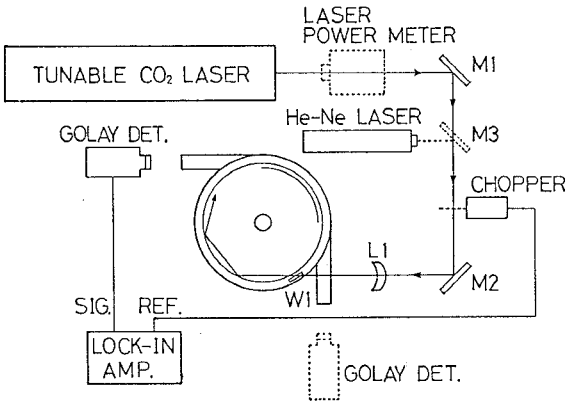

Figure 5. Experimental arrangement.

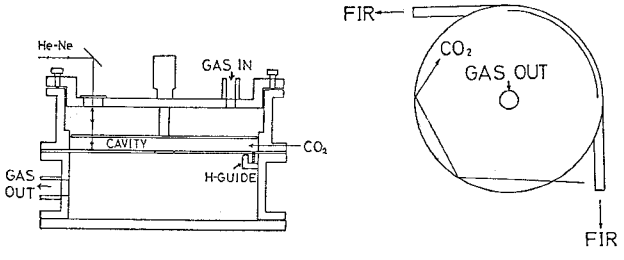

Figure 6. Vertical and horizontal cross-section of the resonator.

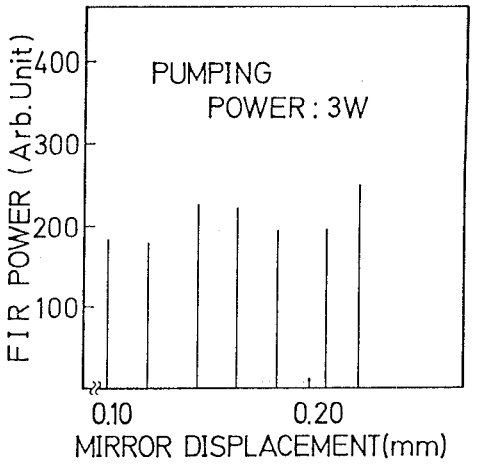

Figure 7. Tuning characteristics.

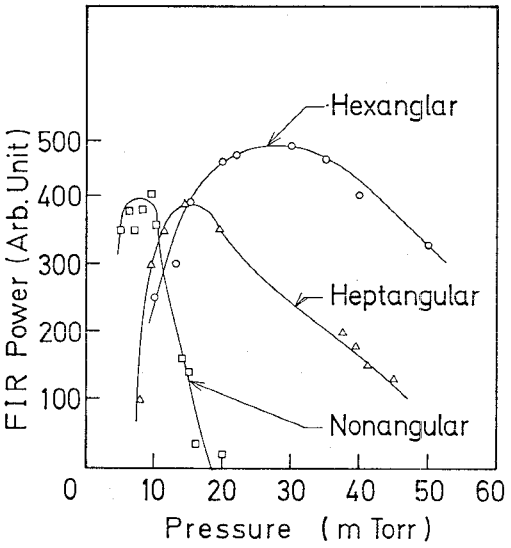

Figure 8. Pressure dependency of FIR output power with parameter of the angle of incidence of pumping light.

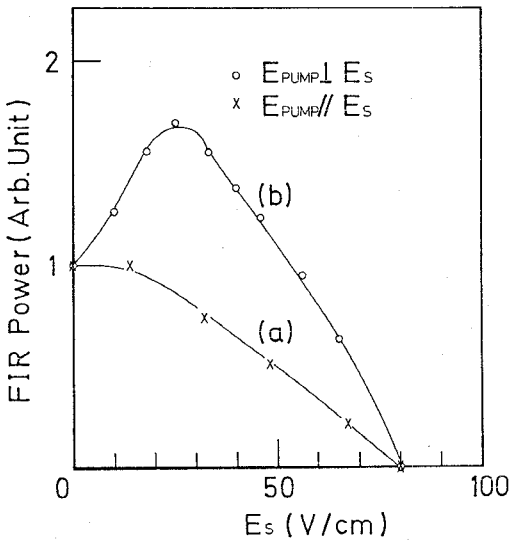

Figure 9. FIR output power as a function of Stark field.